International Journal of Heat and Mass Transfer 106 (2017) 177–182

Contents lists available at ScienceDirect

International Journal of Heat and Mass Transfer

journal homepage: www.elsevier.com/locate/ijhmt

Modification of SIMPLE algorithm to handle natural convection flows with zero-isothermal compressibility

Yutaka Asako [a,*], Mohammad Faghri [b]

[a] Department of Mechanical Precision Engineering, Malaysia-Japan International Institute of Technology, University Technology Malaysia, Jalan Sultan Yahya Petra, 54100 Kuala Lumpur, Malaysia
[b] Department of Mechanical, Industrial and System Engineering, University of Rhode Island, Kingston, RI 02881-0805, USA

ARTICLE INFO

Article history:
Received 15 July 2016
Received in revised form 2 September 2016
Accepted 15 October 2016
Available online 24 October 2016

Keywords:
SIMPLE
Non-Boussinesq approximation
Isothermal compressibility

ABSTRACT

The conventional SIMPLE algorithm for the pressure–velocity coupling has been adopted by many commercial and non-commercial CFD codes. It encounters convergence problem when it is used to solve unsteady natural convection flows with zero-isothermal compressibility. In this paper, a modified version of this algorithm is proposed to remedy this drawback. The modification includes updating of the density at each time step based on its value at the previous time step to satisfy the continuity equation. As an example of utilizing the modified SIMPLE algorithm, the unsteady natural convection in a rectangular cavity with isothermal vertical walls and adiabatic horizontal walls was computed. Physically consistent results were obtained.

1. Introduction

The SIMPLE algorithm [1] for the pressure–velocity coupling has been adopted by many commercial and non-commercial CFD codes such as FLUENT, Star-CD, Phoenix, OpenForm, etc. Both steady and unsteady natural convection in a cavity are solved by this algorithm by using the Boussinesq approximation. This approximation ignores the density changes except for the density that appears in the buoyancy term. It also assumes the density has a linear dependence on temperature. Therefore, Boussinesq approximation is not suitable for simulation of natural convection problems with large temperature changes [2,3] and also large density changes that exist in super critical fluids near pseudo-critical points. Recently, there has been renewed interest in applications which require precise solutions of natural convection in fluids with large variations in density. A numerical simulation using a non-Boussinesq approximation is required where the variable density in all the terms must be considered. There is no difficulty in taking into account the variations in density in the buoyancy term instead of using the assumption of the linear dependence on temperature. However, if the variable density is taken into account in all the terms, the SIMPLE algorithm encounters a convergence problem when it is used to solve unsteady forced convection problems. Matsushita [4] proposed a modification of the outflow boundary condition for an unsteady forced convection in a duct. The treatment of the outflow boundary is modified for the variable density. However, a careful search of the literature failed to disclose any prior work on a natural convection with variable density in a cavity.

This study deals with the modification of SIMPLE algorithm for natural convection for an idealized fluid in a cavity with non-zero isobaric compressibility (coefficient of thermal expansion), $-(\partial\rho/\partial T)_p/\rho$, but with zero-isothermal compressibility, $(\partial\rho/\partial p)_T/\rho$.

The ratio of isothermal to isobaric compressibility for an ideal gas can be expressed as T/p. This ratio is about 0.003 under atmospheric pressure and temperature conditions (10^5 Pa and 300 K). For water, this ratio is about 1.6×10^{-6} [5]. However, for super critical water it is about 3×10^{-6} and is about 6×10^{-6} for carbon dioxide near the pseudo-critical point [5]. Therefore, zero-isothermal compressibility can be assumed under these conditions.

2. An example problem using SIMPLE algorithm

To demonstrate the convergence problem of SIMPLE algorithm, consider an unsteady natural convection in a rectangular cavity with vertical isothermal walls and horizontal adiabatic walls as shown in Fig. 1. All the temperatures are maintained at T_C in the initial state. There is no driving force acting on the fluid and therefore the fluid is assumed to be initially stationary. At $t = 0$, the temperature of the left vertical wall (hot wall) is suddenly raised to T_H from T_C in a stepwise fashion.

* Corresponding author.
E-mail addresses: y.asako@utm.my (Y. Asako), faghrim@uri.edu (M. Faghri).

http://dx.doi.org/10.1016/j.ijheatmasstransfer.2016.10.052
0017-9310/

Nomenclature

a	coefficient of discretization equation
b	source term of discretization equation
C_p	specific heat (W/(kg K))
Ga	Galilei number (–)
H	height of cavity (m)
L	width of cavity (m)
p	pressure (Pa)
P	dimensionless pressure (–)
Pr	Prandtl number (–)
R^C	normalized residual of continuity equation
R^U, R^V	normalized residual of U and V
S_{max}	maximum of rate of mass imbalance in each control volume
S_{sum}	rate of mass imbalance in cavity
t	time (s)
u, v	velocity components (m/s)
U, V	dimensionless velocity components (–)
V	volume integral (m^3)
x, y	coordinates (m)
X, Y	dimensionless coordinates (–)

Greek

β	volume expansivity (1/K)
ϕ	dependent variable
λ	thermal conductivity (W/(m K))
μ	viscosity (Pa s)
ν	kinetic viscosity (m^2/s)
θ	dimensionless temperature (–)
ρ	density (kg/m^3)
ρ^*	dimensionless density (–)
τ	dimensionless time (–)

Subscript

C	cold wall
e, w, n, s	control-volume faces
H	hot wall
nb	neighbor-point
P	central grid point
ref	reference

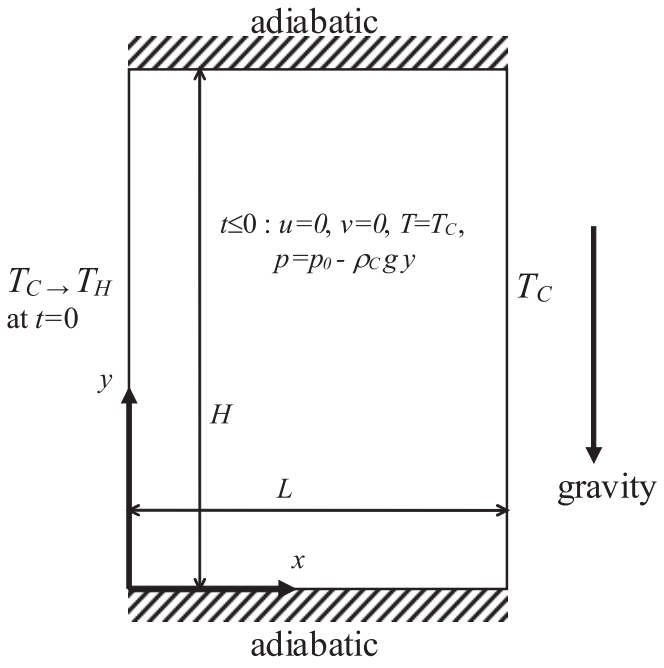

Fig. 1. Natural convection in a rectangular cavity.

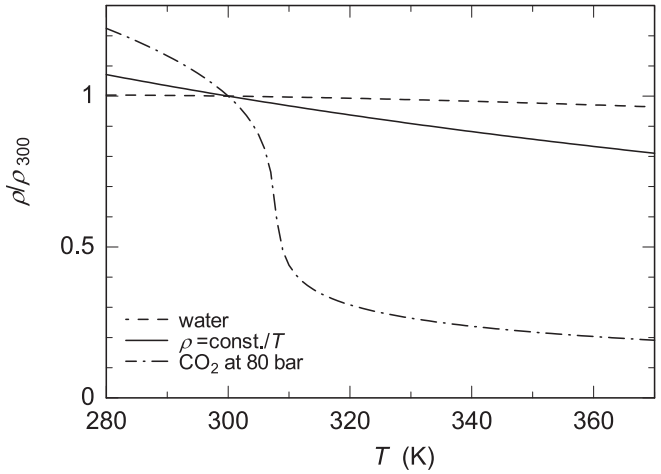

Fig. 2. ρ/ρ_{300} as a function of T.

2.1. Governing equations

The flow in the rectangular cavity is assumed to be two-dimensional. It is further assumed that all the fluid properties except the density are constant and also the fluid density is only a function of temperature as

$$\rho = \frac{const.}{T} \tag{1}$$

The density at a reference temperature, T_{ref}, is denoted by ρ_{ref} and the density ratio is expressed as $\rho/\rho_{ref} = T_{ref}/T$. The density ratio, ρ/ρ_{300} is plotted as a function of T for $T_{ref} = 300$ K in Fig. 2. The variations of the density ratio of water and super critical carbon dioxide at 8 MPa are also plotted in this figure as a reference. As can be seen in this figure, the density change of super critical carbon dioxide near the pseudo-critical point is large.

Under these assumptions, the variable density needs to be taken into account for all the terms and the continuity and the momentum equations can be expressed as:

$$\frac{\partial \rho}{\partial t} + \frac{\partial \rho u}{\partial x} + \frac{\partial \rho v}{\partial y} = 0 \tag{2}$$

$$\frac{\partial \rho u}{\partial t} + \frac{\partial \rho u u}{\partial x} + \frac{\partial \rho u v}{\partial y} = -\frac{\partial p}{\partial x} + \frac{\partial}{\partial x}\left(\mu \frac{\partial u}{\partial x}\right) + \frac{\partial}{\partial y}\left(\mu \frac{\partial u}{\partial y}\right) + \frac{\mu}{3}\frac{\partial}{\partial x}\left(\frac{\partial u}{\partial x} + \frac{\partial v}{\partial y}\right) \tag{3}$$

$$\frac{\partial \rho v}{\partial t} + \frac{\partial \rho u v}{\partial x} + \frac{\partial \rho v v}{\partial y} = -\frac{\partial p}{\partial y} + \frac{\partial}{\partial x}\left(\mu \frac{\partial v}{\partial x}\right) + \frac{\partial}{\partial y}\left(\mu \frac{\partial v}{\partial y}\right) + \frac{\mu}{3}\frac{\partial}{\partial y}\left(\frac{\partial u}{\partial x} + \frac{\partial v}{\partial y}\right) - \rho g \tag{4}$$

The specific enthalpy is expressed as a function of temperature and pressure as (e.g. [6])

$$dh = C_p\, dT + \frac{1-\beta T}{\rho}\, dp \tag{5}$$

where β is the coefficient of thermal expansion and is expressed as

$$\beta = -\frac{1}{\rho}\left(\frac{\partial \rho}{\partial T}\right)_p \tag{6}$$

By substituting Eq. (1) into Eq. (6), this coefficient can be determined to be

$$\beta = \frac{1}{T} \tag{7}$$

Substituting Eq. (7) into Eq. (5), the specific enthalpy of the fluid can be expressed as

$$dh = C_p dT \tag{8}$$

Then, the energy equation can be expressed as

$$\frac{\partial \rho C_p T}{\partial t} + \frac{\partial \rho C_p u T}{\partial x} + \frac{\partial \rho C_p v T}{\partial y} = \frac{\partial}{\partial x}\left(\lambda \frac{\partial T}{\partial x}\right) + \frac{\partial}{\partial y}\left(\lambda \frac{\partial T}{\partial y}\right) \tag{9}$$

Both the viscous dissipation and the substantial derivative of the pressure terms were neglected in Eq. (9) due to low velocities under consideration.

Using the following dimensionless variables:

$$X = \frac{x}{L},\ Y = \frac{y}{L},\ U = \frac{uL}{\nu},\ V = \frac{vL}{\nu},\ P = \frac{p}{\rho_C (\nu/L)^2},$$
$$\tau = \frac{t}{(L^2/\nu)},\ \theta = \frac{T}{T_C},\ \rho^* = \frac{\rho}{\rho_C},\ Ga = \frac{gL^3}{\nu^2},\ Pr = \frac{\nu}{\lambda/(\rho_C C_p)} \tag{10}$$

the dimensionless forms of the governing equations are:

$$\frac{\partial \rho^*}{\partial \tau} + \frac{\partial \rho^* U}{\partial X} + \frac{\partial \rho^* V}{\partial Y} = 0 \tag{11}$$

$$\frac{\partial \rho^* U}{\partial \tau} + \frac{\partial \rho^* UU}{\partial X} + \frac{\partial \rho^* VU}{\partial Y} = -\frac{\partial P}{\partial X} + \frac{\partial^2 U}{\partial X^2} + \frac{\partial^2 U}{\partial Y^2} + \frac{1}{3}\frac{\partial}{\partial X}\left(\frac{\partial U}{\partial X} + \frac{\partial V}{\partial Y}\right) \tag{12}$$

$$\frac{\partial \rho^* V}{\partial \tau} + \frac{\partial \rho^* UV}{\partial X} + \frac{\partial \rho^* VV}{\partial Y} = -\frac{\partial P}{\partial Y} + \frac{\partial^2 V}{\partial X^2} + \frac{\partial^2 V}{\partial Y^2} + \frac{1}{3}\frac{\partial}{\partial Y}\left(\frac{\partial U}{\partial X} + \frac{\partial V}{\partial Y}\right) - Ga\ \rho^* \tag{13}$$

$$\frac{\partial \rho^* \theta}{\partial \tau} + \frac{\partial \rho^* U\theta}{\partial X} + \frac{\partial \rho^* V\theta}{\partial Y} = \frac{1}{Pr}\left\{\frac{\partial^2 \theta}{\partial X^2} + \frac{\partial^2 \theta}{\partial Y^2}\right\} \tag{14}$$

$$\rho^* = \frac{1}{\theta} \tag{15}$$

2.2. Boundary conditions

Temperatures of the walls and the fluid are maintained at T_C when $t < 0$. At $t = 0$, the temperature of the hot wall is suddenly raised to T_H from T_C in a stepwise fashion. Under these assumptions, the dimensionless initial and boundary conditions are expressed as:

$$\begin{aligned}
&\tau < 0 && : \ U = V = 0,\ \theta = 1\\
&\tau \geqslant 0,\ \text{on the hot wall}\ \ (X = 0) && : \ U = V = 0,\ \theta = T_H/T_C\\
&\tau \geqslant 0,\ \text{on the cold wall}\ \ (X = 1) && : \ U = V = 0,\ \theta = 1\\
&\tau \geqslant 0,\ \text{on the horizontal walls} && : \ U = V = 0,\ \partial\theta/\partial Y = 0
\end{aligned} \tag{16}$$

2.3. Numerical computation

The governing equations were discretized using the control volume based power-law scheme of Patankar [1]. All the computations were performed with (122×122) grid points. The grid points were non-uniformly distributed with high concentration of the grids close to the walls. The cell size was gradually increased from the wall in a power-law spacing fashion [7]. The selected index of the power-law spacing was 1.4. The grid size effect on the averaged Nusselt number on the hot wall in the steady state was investigated for a case of $H/L = 2$, $T_H/T_C = 1.133$, $Ga = 5 \times 10^6$ and $Pr = 2$. The corresponding Rayleigh number is about 1.3×10^6. The results are tabulated in Table 1. As can be seen from this table, the grid size effect on Nu_m is small except for the case of coarse grid (22×22).

2.4. Convergence criterion

The following normalized residuals were widely used for the convergence criterion [8]. The normalized residual of U, V, θ is expressed as

$$R^{\phi} = \frac{\sum_{cell\ P} \left|\sum_{nb} a_{nb}\ \phi_{nb} + b - a_P\ \phi_P\right|}{\sum_{cell\ P} |a_P\ \phi_P|} \tag{17}$$

The normalized residual of the continuity equation is

$$R^C = \frac{\sum_{cell\ P} |\text{rate of mass creation in cell } P|}{\text{largest } R^C \text{ in first 5 iteration}} \tag{18}$$

The following rates of mass imbalance are also used for the convergence criterion [1].

$$S_{max} = \max\left(|\text{rate of mass creation in cell } P|\right) \tag{19}$$

$$S_{sum} = \sum_{cell\ P} \text{rate of mass creation in cell } P \tag{20}$$

where S_{sum} expresses the rate of mass imbalance in the cavity and this value must be zero if the mass conservation is to be satisfied.

2.5. Results for the sample computation

The sample computation was conducted for the case of $H/L = 2$, $T_H/T_C = 1.133$, $Ga = 5 \times 10^6$, $Pr = 2$ with the time interval of $\Delta\tau = 10^{-4}$. The convergence criterions used were $R^U < 10^{-5}$ and $R^V < 10^{-5}$. The normalized residuals, R^U, R^V and R^C at $\tau = 10^{-4}$ (the first step) are plotted in Fig. 3 as a function of iteration numbers. As can be seen from this figure, although the normalized residuals, R^U and R^V, decrease with increasing iteration, the normalized residuals of the continuity equation, R^C, does not decrease and it

Table 1
Grid size effect on Nu_m.

Grids	Nu_m	$\frac{Nu_m - Nu_{m\ 122\times122}}{Nu_{m\ 122\times122}} \times 100$
22×22	9.677	0.90%
42×42	9.596	0.06%
82×82	9.587	−0.04%
122×122	9.591	–
162×162	9.594	0.03%
202×202	9.597	0.07%

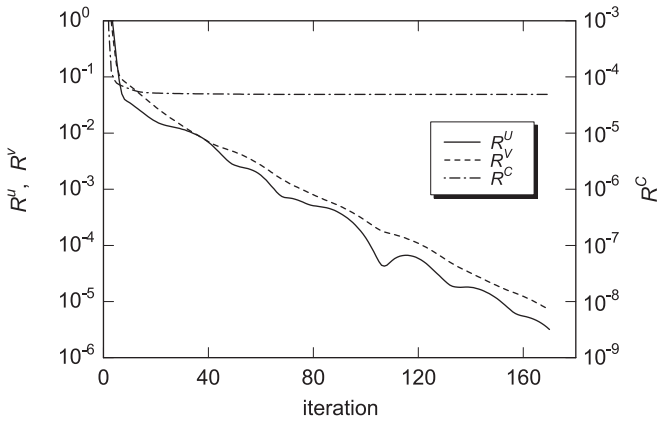

Fig. 3. Normalized residuals R^U, R^V and R^C at $\tau = 10^{-4}$.

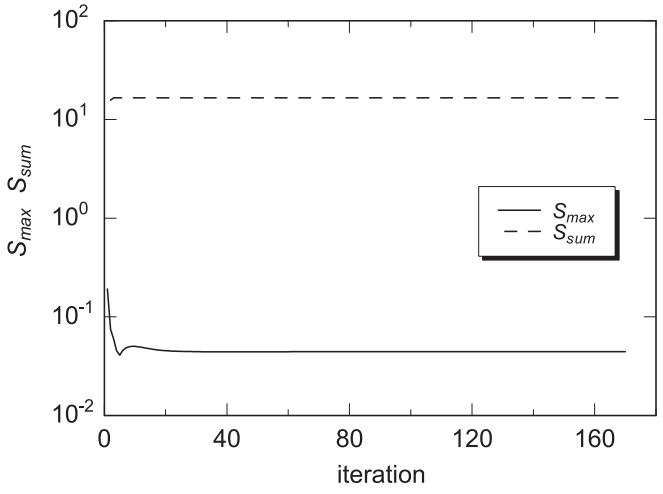

Fig. 4. Rates of mass imbalance S_{max} and S_{sum} at $\tau = 10^{-4}$.

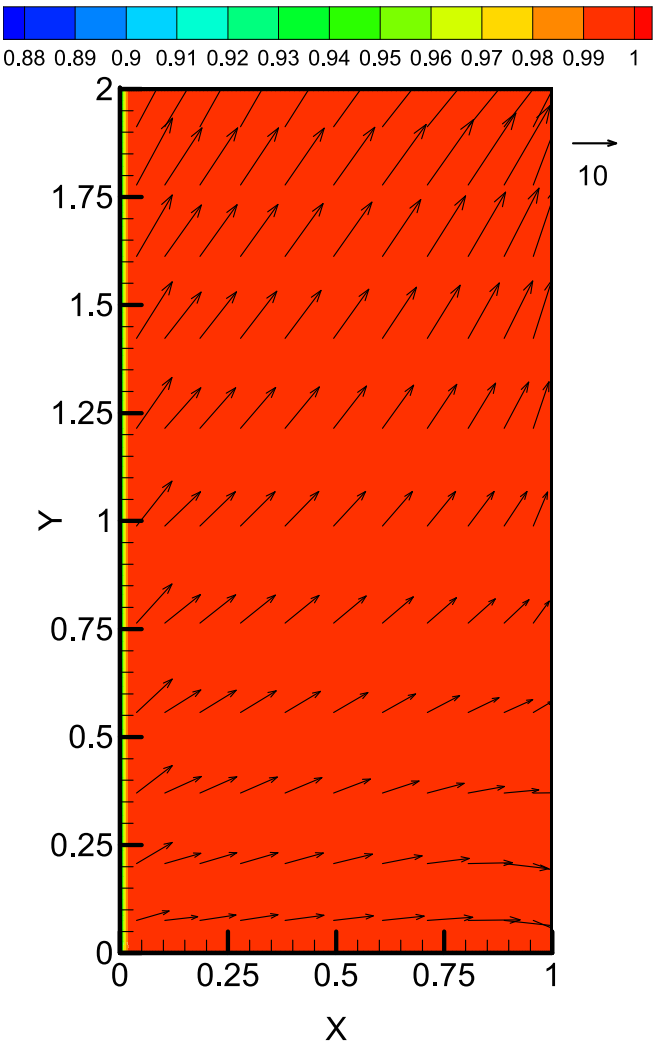

Fig. 5. Velocity vector and contour of dimensionless density ρ^* at $\tau = 10^{-4}$.

remains constant with increasing iteration. The rate of mass imbalance, S_{max} and S_{sum}, are plotted in Fig. 4. As can be seen from this figure, S_{max} and S_{sum} don't decrease and remain relatively constant indicating that the mass conservation is not satisfied in the cavity. The normalized residuals, R^U and R^V, decrease with increasing iteration, although the mass conservation is not satisfied. It is therefore not suitable to use the normalized residuals, R^U and R^V, for the convergence criteria.

The velocity vectors and the contour of the density at $\tau = 10^{-4}$ are plotted in Fig. 5. Since the temperature of the hot wall increases at $\tau = 0$, the fluid temperature in a very thin layer near the hot wall increases. The fluid in the thin layer expands and this results in decrease of the density. As seen in the figure, the fluid $Y = 0.5$ flows upward although the velocity on the walls is zero and the buoyancy force does not work except the thin layer near the hot wall.

The vertical velocity components, V, at $Y = 0.988$ are plotted in Figs. 6 and 7 for $\tau = 10^{-4}$ and 10^{-3}, respectively. As can be seen in Fig. 6, the V values in the whole region from hot to cold wall remain positive at $\tau = 10^{-4}$. In such a case, the mass in the cavity above $Y = 0.988$ should increase. However, as seen in Fig. 5, the fluid density does not increase. Therefore, the velocity profile obtained is physically inconsistent. As seen in Fig. 7, the V in the range of $X > 0.1$ takes negative value. Note that as time advances, a physically consistent velocity profile is obtained.

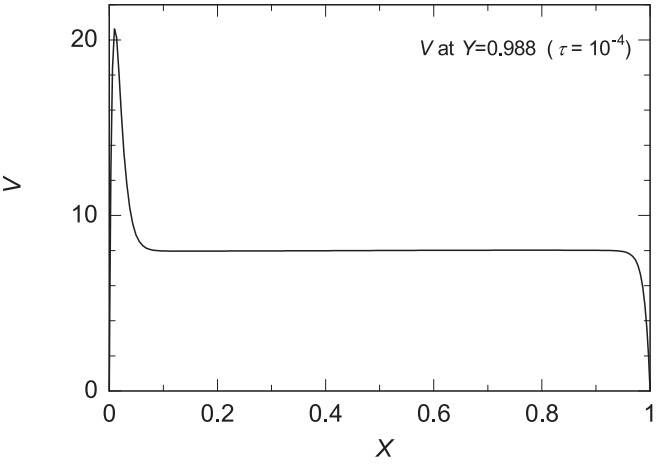

Fig. 6. Velocity profile at $Y = 0.988$ and $\tau = 10^{-4}$.

3. Modification of SIMPLE

Integrating Eq. (2) over the rectangular cavity, the following equation is obtained.

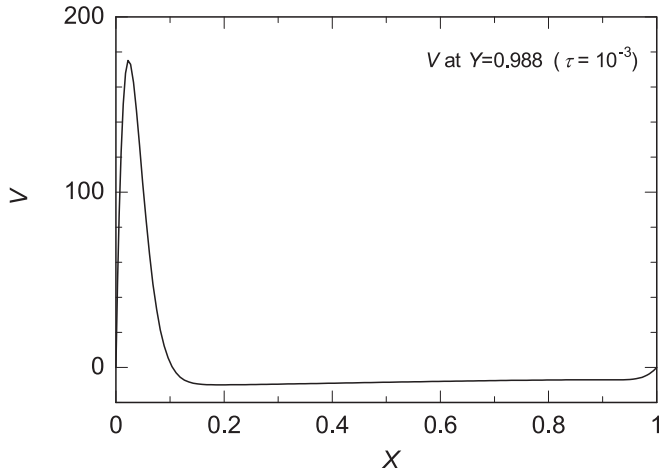

Fig. 7. Velocity profile at $Y = 0.988$ and $\tau = 10^{-3}$.

$$\frac{\partial}{\partial t}\int_V \rho\, dV + \int_S \rho \vec{v} dS = 0 \tag{21}$$

The second term of the above equation vanishes because the velocity is zero on the boundary. Therefore,

$$\frac{\partial}{\partial t}\int_V \rho dV = \frac{\partial M}{\partial t} = 0 \tag{22}$$

where M represents the mass of the fluid in the cavity. Eq. (22) expresses the mass conservation in the cavity. However, in the sample computation, it is assumed that all the temperatures are maintained at T_C in the initial state and at $t = 0$, the temperature of the hot wall is suddenly raised to T_H from T_C in a stepwise fashion. The density of the fluid is only a function of temperature as shown in Fig. 2 and decreases with increasing temperature. In this condition, the temperature of the fluid in the cavity increases with time and this results in a decrease of the fluid density with time. Therefore, the mass conservation is not satisfied under this condition. This is the reason a physically unrealistic velocity profile (Fig. 6) is obtained.

The unsteady term in Eq. (2) is discretized as

$$\frac{\partial \rho}{\partial t} = \frac{\rho - \rho^{old}}{\Delta t} \tag{23}$$

The mass in the cavity can be expressed as

$$M = \sum_{cell\ P} \rho_P\, \Delta V_P,\ M^{old} = \sum_{cell\ P} \rho_P^{old}\, \Delta V_P \tag{24}$$

As mentioned above, the mass conservation is not satisfied under the assumption that the fluid density is only a function of temperature. Therefore, the mass at the new time step is not equal to the mass at the old time step. Therefore, the density at the old time step is modified to satisfy the mass conservation as,

$$\rho^{mod} = \rho^{old}\frac{M}{M^{old}} \tag{25}$$

The modified density at the old time step is used for the pressure correction. The source term of the discretized pressure correction equation is expressed as

$$b = \rho_w u_w^* A_w - \rho_e u_e^* A_e + \rho_s v_s^* A_s - \rho_n v_n^* A_n + \frac{\rho_P^{mod} - \rho_P}{\Delta t}\Delta V_P \tag{26}$$

where u^* and v^* represent the velocity components obtained using the guessed pressure [1]. It is noteworthy that a physically consistent result can be obtained in a case of steady state computation, since the unsteady term of Eq. (2) vanishes and there is no need to modify the density.

4. Results and discussion

A sample computation is performed for the same case as above using the modified SIMPLE algorithm. The computational parameters were $H/L = 2$, $T_H/T_C = 1.133$, $Ga = 5 \times 10^6$, $Pr = 2$ with the time interval of $\Delta\tau = 10^{-4}$. The convergence criterion used was

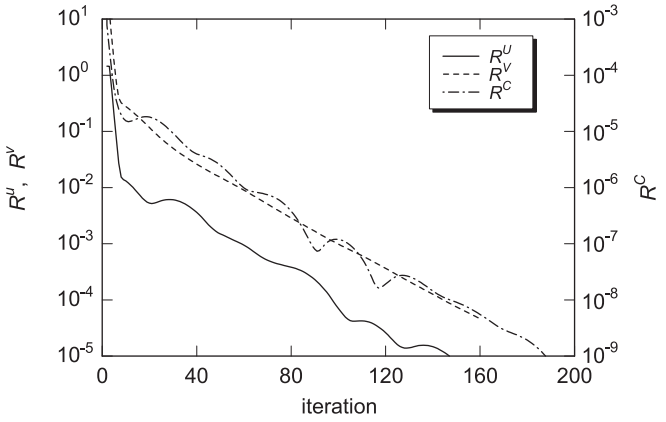

Fig. 8. Normalized residuals R^U, R^V and R^C at $\tau = 10^{-4}$ (modified SIMPLE algorithm).

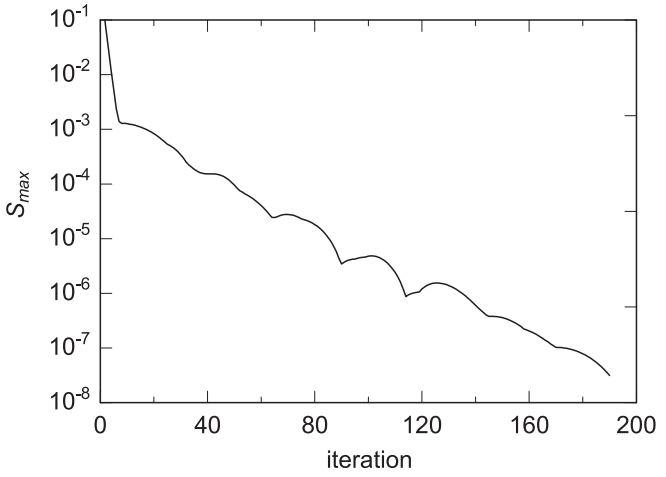

Fig. 9. Maximum rate of mass imbalance S_{max} at $\tau = 10^{-4}$ (modified SIMPLE algorithm).

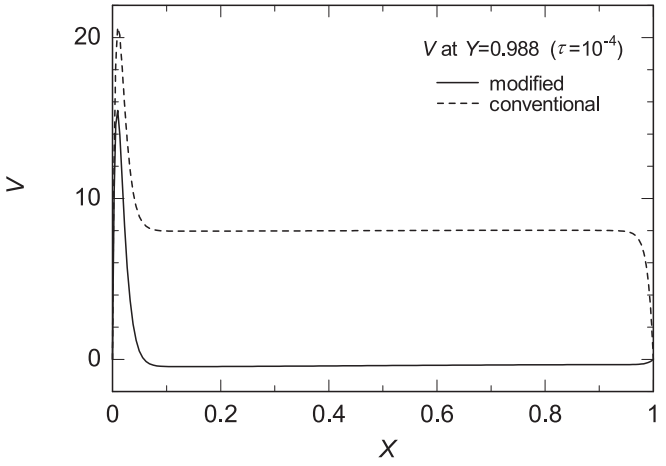

Fig. 10. Comparison of velocity profile at $Y = 0.988$ and $\tau = 10^{-4}$.

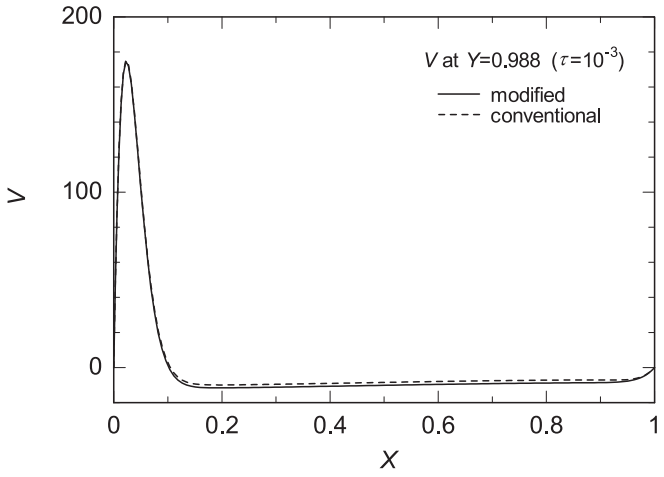

Fig. 11. Comparison of velocity profile at $Y = 0.988$ and $\tau = 10^{-3}$.

$R^C < 10^{-9}$. The normalized residuals, R^U, R^V and R^C at $\tau = 10^{-4}$ (the first step) are plotted in Fig. 8 as a function of iteration numbers. The normalized residuals of the continuity equation, R^C, decreases when the modified density is used. The rate of mass imbalance in the cavity, S_{sum}, takes a value around 10^{-13}. The maximum rate of mass imbalance, S_{max} is plotted in Fig. 9. The S_{max} also decreases with increasing iteration. Therefore, S_{max} or R^C should be used for the convergence criteria. The R^U and R^V are not suitable for the convergence criterions.

The vertical velocity component, V, at $Y = 0.988$ are plotted in Figs. 10 and 11 for $\tau = 10^{-4}$ and 10^{-3}, respectively. The velocity profiles obtained by the conventional SIMPLE are also plotted in these figures. As can be seen in Fig. 10, the velocity profile obtained by the modified SIMPLE algorithm is physically consistent, even at $\tau = 10^{-4}$. As time advances, the difference between the two results decreases.

5. Conclusions

A modified SIMPLE algorithm for the fluids with zero-isothermal compressibility was presented in this paper.

(1) The modification of the density at the old time step was necessary. Physically consistent results were obtained when Eq. (25) was used to modify the density.
(2) The normalized residual of the continuity equation, R^C, or the maximum rate of mass imbalance, S_{max}, must be used for the convergence criterion in the SIMPLE algorithm.

Acknowledgement

The authors would like to thank Dr. Yutaka Okubo, the president of Digital Flow Co. Ltd., for valuable discussion on the convergence criterion.

References

[1] S.V. Patankar, Numerical Heat Transfer and Fluid Flow, Hemisphere Publishing Corporation, New York, 1980, ISBN: 0-89116-522-3.
[2] D.D. Gray, L. Giorgini, Validity of the Boussinesq approximation for liquids and gases, Int. J. Heat Mass Transfer 19 (1975) 545–551.
[3] S. Paolucci, On the Filtering of Sound from the Navier-Stokes Equations, Sandia National Laboratories, 1982, SAND82-8257.
[4] Y. Matsushita, Outflow boundary condition in the finite volume method for unsteady-state fluid flow computation with variable density, Comput. Therm. Sci. 3 (6) (2011) 531–537.
[5] PROPATH group, PROPATH: A Program Package for Thermo-physical Properties of Fluids, Version 13.1, 2008.
[6] Y.A. Cengel, M.A. Boles, Thermodynamics, McGraw-Hill Inc, New Jersey, 1994, ISBN: 0-07-113249-X.
[7] S.V. Patankar, Computation of Conduction and Duct Flow Heat Transfer, Innovative Research Inc, Minnesota, 1991.
[8] ANSYS Inc., ANSYS Fluent 12.0 Use's Guide, 2009.